timates of the annual mean chl-a biomass, the NWLR-Off data yield more realistic estimates of the seasonal variability (i.e., spring and fall blooms) and the expected seasonal cycle in surface chl-a concentrations. This comparison implies that the NWLR filter eliminates high chl-a estimates too severely and retains low chl-a estimates too conservatively (*27*).

10. For the mean chl-a data applied to the 11 NPFAC fishing regions in Table 1, we found the linear regression relation for the NWLR-On and NWLR-Off data to be *chl-a*(NWLR-On) = 0.440 × *chl-a*(NWLR-Off) + 0.523, with r^2 = 0.96 (n = 11 regions; P < 0.0001). For all chl-a data (including the British Columbia data in Table 1), *chl-a*(NWLR-On) = 0.449 × *chl-a*(NWLR-Off) + 0.487 with r^2 = 0.98 (n = 17, all fishing regions; P < 0.0001).
11. Long-term fish catch data are available for the six fishing regions in British Columbia (*7*) for the period 1920 to 1991. The fisheries, particularly for groundfish, were still developing in British Columbia before 1960. Therefore, we calculated the average, long-term catch of resident species for each region for the period 1960 to 1991 (Table 1). The long-term average yield (metric tons km^{-2}) was estimated by dividing the catch by the surface area of each region (*28*).
12. D. M. Ware, G. A. McFarlane, *Can. Spec. Publ. Fish. Aquat. Sci.* **108**, 359 (1989).
13. Table 2 of (*29*) presents observed 10-year mean wind speeds for meteorological buoys moored along the west coast of the United States. Because of the Coriolis effect, winds blowing equatorward parallel to the west coast of North America generate a net seaward transport in the surface Ekman layer. This transport is compensated by a net onshore transport at depth, which gives rise to upwelling conditions over the continental slope.
14. P. T. Strub, P. M. Kosro, A. Huyer, *J. Geophys. Res.* **96**, 14743 (1991).
15. M. J. Perry, J. P. Bolger, D. C. English, in *Coastal Oceanography of Washington and Oregon*, M. R. Landry, B. M. Hickey, Eds. (Elsevier, Amsterdam, 1989), pp. 117–138.
16. T. C. Royer, *J. Geophys. Res.* **87**, 2017 (1982).
17. P. J. Stabeno *et al.*, *Continental Shelf Res.* **24**, 859 (2004).
18. R. W. Tanasichuk, D. M. Ware, W. Shaw, G. A. McFarlane, *Can. J. Fish. Aquat. Sci.* **48**, 2118 (1991).
19. Because there are sufficient data to obtain reasonably accurate estimates of the average annual zooplankton and chl-a concentrations, we were able to divide the six British Columbia fishing regions into 10 smaller subareas. The inset in Fig. 4A shows the relationship between these two variables [*Zoo* = 33.9 × (*chl-a*)$^{0.531}$, adjusted r^2 = 0.81; P = 0.001].
20. E. A. Logerwell, N. Mantua, P. W. Lawson, R. C. Francis, V. N. Agostini, *Fish. Oceanogr.* **12**, 554 (2003).
21. J. A. McGowan, D. R. Cayan, L. M. Dorman, *Science* **281**, 210 (1998).
22. A. J. Richardson, D. S. Schoeman, *Science* **305**, 1609 (2004).
23. S. Tassan, *Applied Optics* **33**, 2369 (1994).
24. K. G. Ruddick, F. Ovidio, M. Rijkeboer, *Applied Optics* **39**, 897 (2000).
25. M. V. H. Lynde, *NOAA Technical Memo., NMFS/NWC-103* (1986).
26. Institute of Ocean Sciences, unpublished data.
27. W. W. Gregg, N. W. Casey, *Remote Sens. Environ.* **93**, 463 (2004).
28. Materials and methods are available as supporting material on *Science* Online.
29. C. E. Dorman, C. D. Winant, *J. Geophys. Res.* **100**, 16029 (1995).
30. Time series of Ekman transport are available from the Pacific Fisheries Environmental Laboratory at www.pfeg.noaa.gov.
31. We thank J. Gower and J. Wallace for providing us with SeaWiFs imagery from the Department of Fisheries and Oceans satellite facility, L. Beauchemin and B. Wallace for processing the SeaWiFS data for the fish catch areas, D. McQueen and S. Romaine for assisting with the zooplankton data, C. Wright and P. Kimber for helping prepare the manuscript, B. Hickey for consulting with us on the validity of variously derived wind fields for the California coastal region, and three reviewers for comments on the manuscript.

Supporting Online Material
www.sciencemag.org/cgi/content/full/1109049/DC1
Materials and Methods
References and Notes

22 December 2004; accepted 15 April 2005
Published online 21 April 2005;
10.1126/science.1109049
Include this information when citing this paper.

REPORTS

An Asymmetric Energetic Type Ic Supernova Viewed Off-Axis, and a Link to Gamma Ray Bursts

Paolo A. Mazzali,[1,2,3,4]* Koji S. Kawabata,[5] Keiichi Maeda,[6] Ken'ichi Nomoto,[1,2]* Alexei V. Filippenko,[7] Enrico Ramirez-Ruiz,[8] Stefano Benetti,[9] Elena Pian,[4] Jinsong Deng,[10,1,2] Nozomu Tominaga,[1] Youichi Ohyama,[11,12] Masanori Iye,[1,13,14] Ryan J. Foley,[7] Thomas Matheson,[15] Lifan Wang,[16] Avishay Gal-Yam[17]

Type Ic supernovae, the explosions after the core collapse of massive stars that have previously lost their hydrogen and helium envelopes, are particularly interesting because of their link with long-duration gamma ray bursts. Although indications exist that these explosions are aspherical, direct evidence has been missing. Late-time observations of supernova SN 2003jd, a luminous type Ic supernova, provide such evidence. Recent Subaru and Keck spectra reveal double-peaked profiles in the nebular lines of neutral oxygen and magnesium. These profiles are different from those of known type Ic supernovae, with or without a gamma ray burst, and they can be understood if SN 2003jd was an aspherical axisymmetric explosion viewed from near the equatorial plane. If SN 2003jd was associated with a gamma ray burst, we missed the burst because it was pointing away from us.

When a massive star reaches the end of its life and exhausts its nuclear fuel, the core itself collapses to form a compact remnant (a neutron star or a black hole). Although the exact mechanism is not well understood, the resulting release of energy leads to the ejection of the envelope of the star at high velocities, producing a supernova (SN).

Typically, a massive star has a large H-rich envelope, making it difficult to observe the innermost part, where the action takes place. However, there are some cases where the H envelope, and also the inner He envelope, were lost before the star exploded, through either a stellar wind or, more likely, binary interaction (*1*). These SNe, called type Ic, offer a view close to the core, and so they are particularly interesting as tools to study the properties of the collapse and of the SN ejection.

Some type Ic SNe, characterized by a very high kinetic energy (*2*, *3*), have been observed to be linked with the previously unexplained phenomenon of gamma ray bursts (GRBs), which are brief but extremely bright flashes of hard (γ-ray and x-ray) radiation that had baffled astronomers for decades (*4*–*8*). The link between type Ic SNe and GRBs is probably not accidental. If a jet is produced by a collapsing star, it can only emerge and generate a GRB if the stellar envelope does not interfere with it (*9*).

In view of this link, we have searched among known type Ic SNe for the counterpart of a property that is typical of GRBs: asphericity. A jet-like explosion is required for GRBs from energetics considerations; if they were spherically symmetric, GRBs would involve excessively large energies, comparable to the rest mass of several suns. The best evidence for asphericity in the GRB-associated SNe (GRB/SNe) to date has come from the fact that iron seems to move faster than oxygen in the ejected material. Evidence of this is seen in spectra obtained several months after the explosion, when the ejected material has decreased in density and behaves like a nebula. The GRB/SN 1998bw (*10*) showed strong emission lines of [O I] (a forbidden line of neutral oxygen), as do normal type Ic SNe, but also of [Fe II] (a forbidden line of singly ionized iron), which are weak in normal type Ic SNe. The [Fe II] lines near 5100 Å in SN 1998bw are broader than the [O I] 6300 and 6363 Å blend.

Asphericity can explain this peculiar situation (*11*). In a typical spherical SN explosion, heavier elements are produced in deeper layers of the progenitor star. As a consequence of the hydrodynamical properties of the explosion, the heavier elements are given less kinetic energy per unit mass than are the external layers, which typically contain lighter elements. However, in a jet-like explosion, the heavier elements (in particular, ^{56}Ni) are probably synthesized near the jet at the time of core collapse and are ejected at high velocities. Lighter elements such as oxygen, which are not produced in the explosion but rather by the progenitor star during its evolution, are ejected near the equatorial plane with a smaller kinetic energy and are distributed in a disc-like structure.

Given this scenario, the observed line profiles depend on the orientation of the explosion with respect to our line of sight. Iron can be observed to be approaching us at a higher velocity than is oxygen, if we view the explosion near the jet direction, which is also the requirement for the GRB to be observed (*10*, *11*). The [O I] line, on the other hand, will appear narrow and sharp in the case of a polar view, because in that case, oxygen moves almost perpendicular with respect to our line of sight (the case of SN 1998bw); however, it will show a broader double-peaked profile for an equatorial view, because a large fraction of the oxygen would then be moving either toward or away from the observer (*11*).

Although this picture seems well established for GRB/SNe, it is important to determine whether it may be common to other type Ic SNe. Measurements of the relative widths of the Fe and O lines are difficult for fainter type Ic SNe because the Fe lines are weak. However, the [O I] line is always rather strong, and it can be expected that given a sufficiently large sample, variations will be seen in its profile reflecting different viewing angles.

Until recently, the evidence for these variations was missing (*12*), but recent observations of SN 2003jd seem to close this gap. SN 2003jd, discovered on 25 October 2003 (*13*) (universal time), is a type Ic SN at a distance of ~80 million parsecs (Mpc) and reached a rather bright maximum. Assuming a galactic extinction $E(B-V)_{\mathrm{Gal}} = 0.06$ magnitudes (mag) (where E is the magnitude difference between the amount of light absorbed in two photometric bands, B is the blue band, and V is the visual band) (*14*), and a host extinction $E(B-V)_{\mathrm{Host}} = 0.09$ mag, as derived from the strength of the interstellar Na I D absorption (*15*), we derive the absolute blue-band magnitude (M_B) at maximum light to be $M_B(\mathrm{max}) \approx -18.7$ mag. This is much more luminous than the normal type Ic SN 1994I (*1*, *16*) and is comparable to the GRB/SNe 1998bw (*4*) and 2003dh (*6*). Spectroscopically, however, SN 2003jd shows narrower lines than the hyper-energetic GRB/SNe (Fig. 1), and it appears to be intermediate between those and the normal type Ic SN 1994I (*16*). The closest analog may be the energetic SN 2002ap (*17*, *18*).

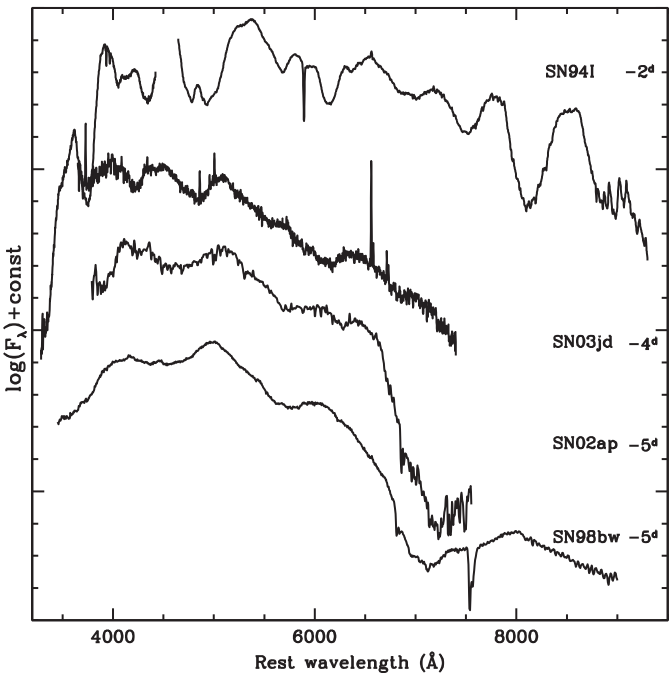

Fig. 1. The near-maximum optical spectrum of SN 2003jd compared with spectra of other type Ic SNe at a similar phase (F_λ is the flux per unit wavelength). The dates are the days relative to the optical maximum (i.e., the minus sign means before the maximum light). Spectra are ordered by increasing line width (implying increasing kinetic energy per unit mass), ranging from the normal SN 1994I (*16*), to the energetic SN 2002ap (*17*, *18*), to the hyper-energetic GRB/SN 1998bw (*30*). The absorption line near 7600 Å in the spectrum of SN 1998bw is telluric.

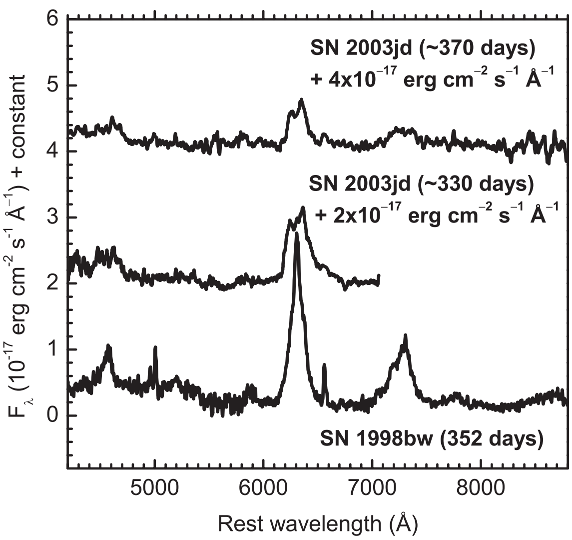

Fig. 2. Nebular spectra of type Ic SNe. The bottom curve shows the nebular spectrum of SN 1998bw (*30*) taken 337 days after maximum light (352 days after the explosion). Note the Mg I], [Fe II], [O I], and [Ca II] lines near 4570, 5100, 6300, and 7300 Å, respectively. The middle curve shows the Subaru FOCAS spectrum of SN 2003jd ~330 days after the putative time of explosion. The top curve shows the Keck spectrum of SN 2003jd at an epoch of ~370 days. The [O I] 6300, 6363 Å line in SN 2003jd clearly exhibit a double-peaked profile. Marginal evidence of a double peak is also present in the profiles of Mg I] at 4570 Å and [Ca II] at 7300 Å. The spectrum of SN 1998bw has been shifted in flux to make it consistent with the distance of SN 2003jd.

[1]Department of Astronomy, [2]Research Center for the Early Universe, School of Science, University of Tokyo, Bunkyo-ku, Tokyo 113-0033, Japan. [3]Max-Planck-Institut für Astrophysik, Karl-Schwarzschild Strasse 1, D-85748 Garching, Germany. [4]Instituto Nazionale di Astrofisica (INAF)-Osservatorio Astronomico di Trieste, Via Tiepolo 11, I-34131 Trieste, Italy. [5]Hiroshima Astrophysical Science Center, Hiroshima University, Hiroshima 739-8526, Japan. [6]Department of Earth Science and Astronomy, Graduate School of Arts and Sciences, University of Tokyo, Komaba 3-8-1, Meguro-ku, Tokyo 153-8902, Japan. [7]Department of Astronomy, University of California, Berkeley, CA 94720–3411, USA. [8]Institute for Advanced Study, Einstein Drive, Princeton, NJ 08540, USA. [9]INAF-Osservatorio Astronomico di Padova, vicolo del'Osservatorio 5, 35122 Padova, Italy. [10]National Astronomical Observatories, CAS, 20A Datun Road, Chaoyang District, Beijing 100012, China. [11]Department of Infrared Astrophysics, Institute of Space and Astronautical Science, Japan Aerospace Exploration Agency, 3-1-1 Yoshinodai, Sagamihara, Kanagawa, 229-8510, Japan. [12]Subaru Telescope, National Astronomical Observatory of Japan (NAOJ), 650 North A'ohoku Place, Hilo, HI 96720, USA. [13]Optical and Infrared Astronomy Division, National Astronomical Observatory, Mitaka, Tokyo 181-8588, Japan. [14]Department of Astronomical Science, School of Physical Sciences, Graduate University for Advanced Studies, Osawa, Mitaka, Tokyo 181-8588, Japan. [15]National Optical Astronomy Observatory, 950 North Cherry Avenue, Tucson, AZ 85719–4933, USA. [16]Lawrence Berkeley National Laboratory, 50-232, 1 Cyclotron Road, Berkeley, CA 94720, USA. [17]Department of Astronomy, California Institute of Technology, Pasadena, CA 91125, USA.

*To whom correspondence should be addressed. E-mail: mazzali@ts.astro.it (P.A.M.); nomoto@astron.s.u-tokyo.ac.jp (K.N.)

We observed SN 2003jd in the nebular phase with the Japanese 8.2-m Subaru telescope on 12 September 2004 (*19*) using the Faint Object Camera and Spectrograph (FOCAS) (*20*), and with the 10-m Keck-I telescope on 19 October 2004 using the Low Resolution Imaging Spectrograph (LRIS) (*21*). These dates correspond to SN ages of ~330 and ~370 days after explosion, respectively. In both spectra (Fig. 2), the nebular line [O I], at wavelengths of 6300 and 6363 Å, clearly has a double-peaked profile with full width at half maximum (FWHM) ≈ 8000 km s^{-1}. The semiforbidden Mg I] line at 4570 Å shows a similar profile. Magnesium is formed near oxygen in the progenitor star. The [Fe II] blend near 5100 Å is quite weak.

Late-phase emission is created by the release of the heat deposited by γ rays and positrons, both of which are emitted in the decay chain ^{56}Ni → ^{56}Co → ^{56}Fe. Therefore, the mass of ^{56}Ni can be determined indirectly through the strength of the emission lines. Because SN 2003jd was not as luminous as SN 1998bw, we rescaled the synthetic spectra to the appropriate ^{56}Ni mass, the best value for which was ~0.3 the mass of the Sun ($M_\odot$). This value is actually very similar to that derived for the GRB/SN 2003dh (*22*, *23*) and much larger than in the non-GRB type Ic SNe (*17*).

We computed nebular spectra of two-dimensional (2D) explosion models for various asphericities and orientations (*11*). We found that a spherical model produces a flat-topped [O I] profile, which is not compatible with either SN 1998bw or SN 2003jd. The flat-topped emission is a typical characteristic of emission from a shell. Indeed, the emission from any spherically distributed material should have a maximum at the wavelength of the line transition between 6300 and 6363 Å, taking into account the line blending. On the other hand, Fig. 3 shows that a highly aspherical model can explain the [O I] line profiles in both SN 1998bw and SN 2003jd. To reproduce the double-peaked profile of the [O I] line in SN 2003jd, we found that SN 2003jd must be oriented ≳70° away from our line of sight. In contrast, for SN 1998bw, this angle was only ~15° to 30° (*11*), and it was even smaller for SN 2003dh (*24*). Less aspherical models do not produce sufficiently sharp [O I] in SN 1998bw.

This result confirms that SN 2003jd was a highly aspherical explosion, and it raises the interesting question of whether SN 2003jd was itself a GRB/SN. A GRB was not detected in coincidence with SN 2003jd (*25*).

If the explosion was very off-axis, we presume that we would not have been able to detect γ rays. However, a GRB is expected to produce a long-lived radiative output through synchrotron emission. X-ray and radio emissions are produced by the deceleration of the relativistic jet as it expands into the wind emitted by the progenitor star before it exploded. This afterglow emission is very weak until the Doppler cone of the beam intersects our line of sight, making off-axis GRB jets directly detectable only months after the event, and at long wavelengths.

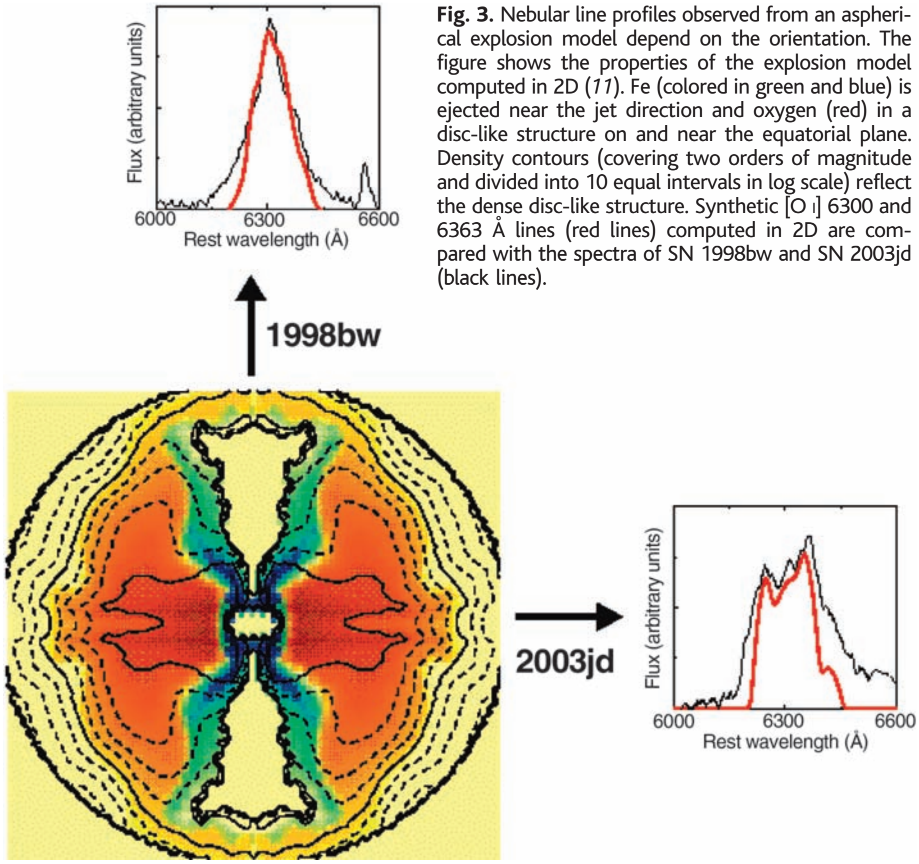

Fig. 3. Nebular line profiles observed from an aspherical explosion model depend on the orientation. The figure shows the properties of the explosion model computed in 2D (*11*). Fe (colored in green and blue) is ejected near the jet direction and oxygen (red) in a disc-like structure on and near the equatorial plane. Density contours (covering two orders of magnitude and divided into 10 equal intervals in log scale) reflect the dense disc-like structure. Synthetic [O I] 6300 and 6363 Å lines (red lines) computed in 2D are compared with the spectra of SN 1998bw and SN 2003jd (black lines).

SN 2003jd was observed in x-rays with Chandra on 10 November 2004, about 30 days after the explosion, and was not detected to an x-ray limit $L_X \leq 3.8 \times 10^{38}$ erg s^{-1} in the energy interval 0.3 to 2 keV (*26*). It was also observed in the radio regime (8.4 GHz) 9 days after the explosion, and again not detected to a radio limit $L_R \leq 10^{27}$ erg s^{-1} Hz^{-1} (*27*).

These nondetections may suggest that SN 2003jd did not produce a GRB. However, absence of evidence is not necessarily evidence of absence. Let us consider the standard jet associated with typical GRBs, that is, a sharp-edged uniform jet with $E = 10^{51}$ erg and a 5° opening angle, expanding laterally at the local sound speed (see Fig. 4 legend for other parameters) (*28*, *29*). If the jet expands in a wind with density $\dot{M}/v = 5 \times 10^{11}$ g cm^{-1} (for example, a mass-loss rate $\dot{M} = 10^{-6}$ $M_\odot$ per year and velocity v = 2000 km s^{-1}), it would give rise to the x-ray and radio light curves shown in Fig. 4. If the SN made a large angle (≥60°) with respect to our line of sight, its associated GRB jet, if present, would not have been detected in the x-rays or radio. Furthermore, the afterglow emission can be fainter for a lower jet energy and/or for a lower wind density.

Although this does not by itself prove that SN 2003jd produced a GRB, it is certainly a possibility, because quantities such as the ejected mass of ^{56}Ni are comparable to those typical of GRB/SNe (*22*). Moreover, our observations confirm that the energetic SN 2003jd is an aspherical explosion, reinforcing the case for a link with a GRB. It could also be the case for other energetic type Ic SNe. The lack of x-ray and radio emission does not place stringent constraints on the intrinsic kinetic energy carried by the SN as long as the ejecta experience little deceleration before ~30 days. The expansion velocity (which need not be isotropic) must be $\lesssim 0.2\ A_*^{-1/3}\ (\varepsilon_e/0.1)^{-1/3} c$ (where ε_e is the fraction of the total blast energy that goes into shock-accelerated electrons, A_* is wind density ($\dot{M}/v$), and c is the speed of light) in order to produce L_X ($t \approx 30$ days) ≤ 3.8×10^{38} erg s^{-1} for a standard 10^{51}-erg SN shell expanding into a wind with density $A_* = (\dot{M}/v)/(5 \times 10^{11}\ \mathrm{g\ cm^{-1}}) = 1$ (*28*). The average expansion velocity along our line of sight can be estimated from the early-time spectra; for SN 2003jd, this is about 0.05c. In an aspherical explosion, however, the kinetic energy must be considerably larger near the rotation axis of the stellar progenitor, with bulk expansion velocities close to ~0.1c.

The bright SN 2003jd is the first type Ic SN that shows double peaks in the [O I] line (*12*), which suggests that the degree of asphericity is

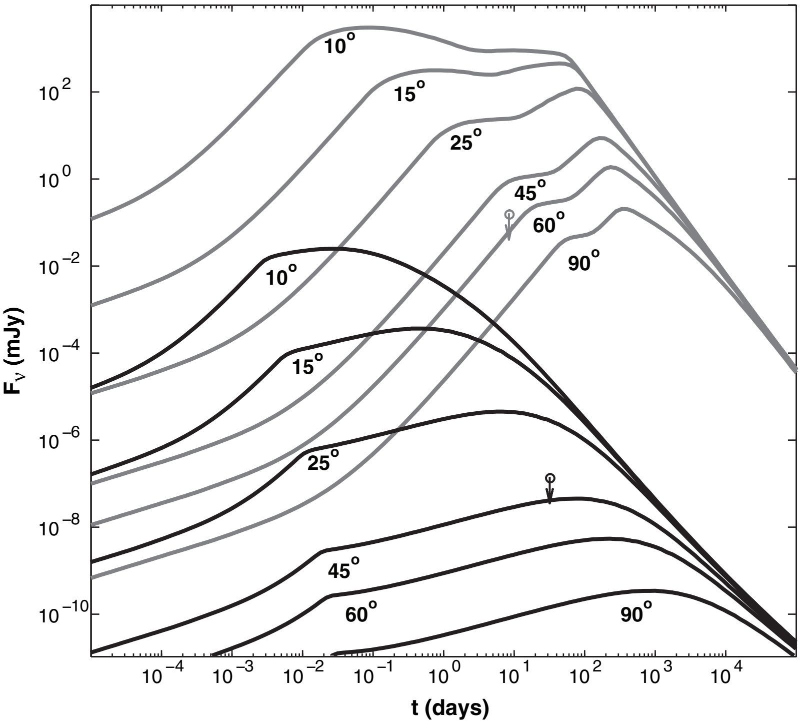

Fig. 4. Afterglow emission from a sharp-edged uniform jet in SN 2003jd. X-ray (0.3 to 2 keV, black) and radio (8.4 GHz, gray) light curves are calculated for various viewing angles, θ_{obs}, for a GRB with the standard parameters $E_{jet} = 10^{51}$ erg, $\varepsilon_e = 0.1$, $\varepsilon_B = 0.1$, $\theta_0 = 5°$, and $A_* = 1$ (where E_{jet} is the energy in the jet, ε_e and ε_B are the fraction of the internal energy in the electrons and magnetic field, respectively, and θ_0 is the opening half-angle of the jet). The synchrotron spectrum is taken to be a piecewise power law with the usual self-absorption, cooling, and injection frequencies calculated from the cooled electron distribution and magnetic field (*28*, *29*). The observed radio and x-ray upper limits for SN 2003jd are marked by open circles. Cosmological parameters taken in the model are $\Omega_m = 0.27$, $\Omega_\Lambda = 0.73$, and $H_0 = 72$ km s^{-1} Mpc^{-1}, where Ω_m is the matter density of the universe, Ω_Λ is the energy density of the universe, and H_0 is the Hubble constant.

not the same in all type Ic SNe. The GRB/SNe 1998bw and 2003dh, which are probably highly aspherical, have been discovered thanks to a GRB trigger; their orientation is therefore such that the [O I] profile must be single-peaked. For normal type Ic SNe, which are on average closer and easier to discover, the lack of observed double-peaked profiles suggests that they are not as strongly aspherical. SN 2003jd appears to share many of the properties (energetics and luminosity) of the GRB/SNe, but it was discovered independent of a GRB, and it is likely to be an aspherical SN viewed off-axis. There have been three energetic type Ic SNe without a GRB trigger (therefore less biased)—SNe 1997dq, 1997ef, and 2002ap—whose nebular spectra did not show the double peaks in the [O I] 6300 Å line. Given the small sample, the number (one out of four) is not inconsistent with our interpretation that the viewing angle $\gtrsim 70°$ results in the double-peaked [O I].

Additional sensitive radio and x-ray observations of SN 2003jd are strongly encouraged, because a jet with the standard parameters could still be detectable by deep observations (Fig. 4). The result should provide valuable tests for the presence of an off-axis GRB with the typical parameters and would further constrain the viewing angle and the mass-loss rate.

References and Notes

1. K. Nomoto *et al.*, *Nature* **371**, 227 (1994).
2. K. Iwamoto *et al.*, *Nature* **395**, 672 (1998).
3. K. Nomoto *et al.*, in *Stellar Collapse*, C. L. Fryer, Ed. (Kluwer Academic, Dordrecht, Netherlands, 2004), pp. 277–325.
4. T. J. Galama *et al.*, *Nature* **395**, 670 (1998).
5. C. Stanek *et al.*, *Astrophys. J.* **591**, L17 (2003).
6. T. Matheson *et al.*, *Astrophys. J.* **599**, 394 (2003).
7. J. Hjorth *et al.*, *Nature* **423**, 847 (2003).
8. J. Malesani *et al.*, *Astrophys. J.* **609**, L5 (2004).
9. A. E. MacFadyen, S. E. Woosley, *Astrophys. J.* **524**, 262 (1999).
10. P. A. Mazzali *et al.*, *Astrophys. J.* **559**, 1047 (2001).
11. K. Maeda *et al.*, *Astrophys. J.* **565**, 405 (2002).
12. T. Matheson *et al.*, *Astron. J.* **121**, 1648 (2001).
13. J. Burket, B. Swift, W. Li, *Int. Astron. Union Circ.* **8232** (2003).
14. D. Schlegel, D. Finkbeiner, M. Davis, *Astrophys. J.* **500**, 525 (1998).
15. S. Benetti *et al.*, in preparation.
16. A. V. Filippenko *et al.*, *Astrophys. J.* **450**, L11 (1995).
17. P. A. Mazzali *et al.*, *Astrophys. J.* **572**, L61 (2002).
18. R. J. Foley *et al.*, *Publ. Astron. Soc. Pac.* **115**, 1220 (2003).
19. K. Kawabata *et al.*, *Int. Astron. Union Circ.* **8410** (2004).
20. N. Kashikawa *et al.*, *Publ. Astron. Soc. Jpn.* **54**, 819 (2002).
21. J. B. Oke *et al.*, *Publ. Astron. Soc. Pac.* **107**, 375 (1995).
22. P. A. Mazzali *et al.*, *Astrophys. J.* **599**, L95 (2003).
23. J. Deng *et al.*, *Astrophys. J.* **624**, 898 (2005).
24. E. Ramirez-Ruiz *et al.*, in press (http://arxiv.org/abs/astro-ph/0412145).
25. K. Hurley *et al.*, *GRB Coord. Network Circ. Serv.* **2003**, no. 2439 (2003).
26. D. Watson, E. Pian, J. N. Reeves, J. Hjorth, K. Pedersen, *GRB Coord. Network Circ. Serv.* **2003**, no. 2445 (2003).
27. A. M. Soderberg, S. R. Kulkarni, D. A. Frail, *GRB Coord. Network Circ. Serv.* **2003**, no. 2435 (2003).
28. E. Ramirez-Ruiz, P. Madau, *Astrophys. J.* **608**, L89 (2004).
29. J. Granot, E. Ramirez-Ruiz, *Astrophys. J.* **609**, L9 (2004).
30. F. Patat *et al.*, *Astrophys. J.* **555**, 900 (2001).

31. This work is based on data collected at the Subaru telescope, operated by the NAOJ, and at the Keck telescopes made possible by the W. M. Keck Foundation. This research is supported in part by the Japan Society for the Promotion of Science and the Ministry of Education, Culture, Sports, Science, and Technology in Japan and by NSF in the USA. E.R.-R. is a Chandra Fellow and A.G.-Y. is a Hubble Fellow.

22 February 2005; accepted 18 April 2005
10.1126/science.1111384

Scaling in the Time Domain: Universal Dynamics of Order Fluctuations in Fe_3Al

Cristian Mocuta,[1]* Harald Reichert,[1]† Klaus Mecke,[1]‡ Helmut Dosch,[1,2] Michael Drakopoulos[3]§

By focusing a highly brilliant synchrotron x-ray beam to a micrometer spot on a sample, we measured in real time the x-ray intensity fluctuations associated with order fluctuations in crystalline materials. We applied this method to the binary alloy Fe_3Al near its continuous A2-B2 phase transformation and determined a specific four-point time correlation function for the order parameter. From a detailed theoretical analysis, dynamical scaling in the time domain with a transition from noncritical to critical dynamics is disclosed.

A premier objective of condensed matter research is to understand and predict how a material reacts upon external fields—such as temperature, pressure, and magnetic or electric fields—especially near a phase transition. The macroscopic response functions χ